EVS27
Barcelona, Spain, November 17-20, 2013

Influence of Current and Temperature Variation on a $LiFePO_4$ Battery Total Capacity

Andrea Marongiu[1,3], Thapakorn Pavanarit[1,3], Dirk Uwe Sauer[1,2,3]
[1] *Electrochemical Energy Conversion and Storage Systems Group - Institute for Power Electronics and Electrical Drives (ISEA), RWTH Aachen University, Jägerstrasse. 17/19, 52066 Aachen, Germany, Email: batteries@isea.rwth-aachen.de*
[2] *Institute for Power Generation and Storage Systems (PGS), E.ON ERC, RWTH Aachen University, Germany*
[3] *Jülich Aachen Research Alliance, JARA-Energy, Germany*

Abstract

Due to the dynamic conditions during the driving operation with rarely deep discharging, the on-board evaluation of the total capacity of the battery pack in a plug-in hybrid electric vehicle (PHEV) and electric vehicle (EV) is one of the most challenging tasks of a battery management system (BMS). In fact, the rapid dynamic variation of the current rate, the unsteady ambient temperature and stand stills of variable duration yield to a situation completely different in respect of the one met in the laboratory (i.e. constant continuous current discharge with a constant ambient temperature). The aim of this paper is to investigate the influence of current rate and temperature variation on the final total capacity that a lithium iron phosphate ($LiFePO_4$) battery is able to deliver. The effect on the total capacity of current and temperature is deeply investigated, both for a cell in a new and aged state: the current and the temperature have been changed during the discharge process continuously in a systematic manner, in order to prove if these factors influence not only the last part of the discharge process but also the early one. The execution of the same tests for cells in different aged state allows the comparison of the results and the identification of the factor influence variation with the battery lifetime. At the end, the repercussions that the current and temperature variation have in the online calculation of the actual total battery capacity are discussed, and a possible implementation for EVs and PHEVs on-board algorithm for capacity estimation is illustrated.

Keywords: $LiFePO_4$ battery, Online capacity estimation, Total battery capacity, Battery Management System algorithm

1 Introduction

The increasing attention towards the environmental issue and the growing limited availability of resources have recently led to several investigations on lithium-ion batteries as the possible key solution for PHEVs and EVs, thanks to their excellent energy density characteristics and cycle-lifetimes of more than thousand cycles [1]. The BMS performs a fundamental role in the management of a battery pack in a vehicle. One of its main tasks is to measure the actual total capacity of the battery and evaluate the decreasing of this parameter during the whole battery lifetime, due to the aging effects.

Generally the total capacity a battery is able to deliver is measured with a process led at ambient temperature (20-25 °C) composed by a fully charge phase followed by a total discharge phase with a constant current of 1C (current corresponding to the nominal capacity), which is stopped when the cell reaches the characteristic cut-off voltage. The final total capacity value is obtained integrating the current with respect to the time. As it can easily be understood, such conditions are completely prohibitive in PHEVs or EVs, firstly because the temperature and the current rate change continuously during the operating conditions (Figure 1), and secondly because the battery pack is rarely or never discharged to the complete empty state.

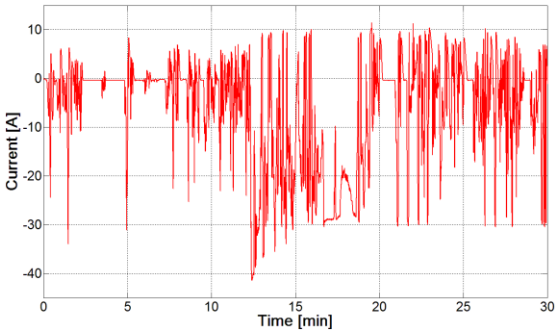

Figure 1: Example of battery current profile obtained driving an electric vehicle and scaled for an 8 Ah high power lithium-ion cell.

Recently several researches have been focused on this topic, but the information about the influence of the current and temperature variation on the total capacity are limited. Shen et al. [2] proposed a method suitable to estimate only the available capacity of a lead acid battery in a certain time in presence of a variable discharge current, according to the terminal voltage and to the predefined cut-off voltage. Roscher et al. [3] have studied the power capability of a $LiFePO_4$ battery through pulse tests and partial cycle test, in order to evaluate the impact of the past history on the internal resistance. Concerning the algorithm ideas used to detect the total capacity, most of the methodologies employed base on an amp-hour calculation between two predefined states of charge (SOCs) [4]. Einhorn et al. [5] have evaluated the oscillation of the calculated value depending of the value of the two SOCs. Plett et al. [6] improved the methodology using a weighted total least square algorithm, to obtain a more precise capacity value. Tang et al. [7] calculated the two values of SOC towards the use of an equivalent circuit model for the battery examined, while Rosca et al. [8] have implemented the method by means of an Extended Kalman Filter. Zheng et al. [9] have measured the actual capacity value of a battery pack studying the behavior during the charging process, however to let the algorithm work properly a complete charging process starting from a fully discharged state is needed.

This work presents how the variation of current rate and temperature during the discharge process influence the final capacity value of a lithium iron phosphate ($LiFePO_4$) battery, and discuss how this influence can be implemented in EVs and PHEVs on-board algorithm for total capacity estimation. The investigation is carried out for two cells, one completely new and one in a significantly aged state, in order to observe how the current and temperature variation dependency change with the battery lifetime. The paper is structured as follows. Chapter 2 show the characteristic of the tested cells and the test matrix followed during the investigation. In chapter 3 the test results are analyzed and the different behavior between the new and aged cell is evaluated. In chapter 4 a possible implementation of the observed results in an algorithm for online capacity estimation is considered and discussed. Chapter 5 closes the work with the conclusion.

2 Experimental

As already mentioned in the introduction, tests on two $LiFePO_4$ cells in different aging state have been carried out. The cells are produced by OMT GmbH, they are high power $LiFePO_4$ cells with a nominal capacity of 8 Ah, a maximum voltage of 3.65 V, a cut-off voltage of 2 V and a maximum continuous discharge current of 200 A (corresponding to 25C). An overview of the cells investigated and their past history is shown in Table 1. The tests have been performed using a battery test bench system manufactured by Digatron [10] (with a maximum charge/discharge current of 200 A, current regulation accuracy of ±0.5% and resolution of 15 bit) and temperature chambers manufactured by Binder [11].

The tests can be grouped in three categories: tests to investigate the current and the temperature variation dependency and tests to investigate the presence of pause during the discharge process. In the next subsections the procedure used for the tests is introduced. In each table, the value of the SOC is referred to the actual battery capacity, while the value of the current during the discharge process (C rate) is referred to the battery nominal capacity.

Table 1: Overview of the cells used during the measurements

Cell Name	Present capacity/Initial capacity	Aging history
Cell A	8.8 Ah/8.2 Ah	New Cell.
Cell B	7.207 Ah/8.16 Ah	Significantly aged cell after 1312 equivalent full cycles at 30 °C with 10% DOD, SOC average of 50% and current rate of 3C.

2.1 Tests for Current Variation Dependency

The aim of these tests was to investigate the influence of the current rate variation during the discharge process on the total final capacity that the battery was able to deliver and particularly to demonstrate 1) if this variation conditions only influenced the last part or the whole discharge process, and 2) if the aging state was a critical factor. The tests were divided in four parts, and were carried out for two cells in different aged state. Table 2 shows the first part of the test.

Table 2: Test matrix for current variation investigation with two steps (1st step: 100% → 50% SOC. 2nd step: 50% → 0% SOC)

Test Nr.			Current [C rate]	
0 °C	23 °C	40°C	100%→50%	50%→Empty%
1	7	13	0.2C	1C
2	8	14	1C	0.2C
3	9	15	0.2C	5C
4	10	16	5C	0.2C
5	11	17	1C	5C
6	12	18	5C	1C

Firstly, reference tests have been carried out, discharging the battery from a fully charged state to the empty state (cut-off voltage) with a constant current rate, with three different values (0,2C - 1C – 5C): the aim was to have a reference in respect of discharge process with inconstant discharge current. Afterwards, in the next test, the battery started in a fully charged state, and then it was discharged from 100% to 50% SOC with a current I_1, and from 50% SOC to the empty state (cut-off voltage) with a current I_2 different to I_1. Afterwards the test was repeated with inverted current values. The tests were carried out for three different current rates (0.2C - 1C - 5C) and for three different temperatures (0 - 23 - 40°C). Moreover, as already mentioned before, the tests were conducted for two batteries in different aged states: taking into account that the nominal battery capacity is 8 Ah, the new cell (Cell A) has shown during the reference tests an initial total capacity of 8.199 Ah (102.4%), while the aged cell has shown an initial total capacity of 7.207 Ah (90%).

Table 3 shows a portion of the second part of the tests.

Table 3: Portion of the test matrix for current variation investigation with three steps (1st step: 100% → 66% SOC - 2nd step: 66% → 33% SOC – 3rd step: 33% → 0% SOC). Test done for ambient temperature of 23 °C

Nr.	Current [C rate]		
	100%→66%	66%→33%	33%→Empty
19	0.2C	1C	5C
20	0.2C	5C	1C
21	1C	0.2C	5C
22	1C	5C	0.2C
23	5C	0.2C	1C
24	5C	1C	0.2C

The routine was the same as for the precedent tests, with the difference that in this case the procedure consisted of discharging the battery in three steps with three different current rates and for an ambient temperature of 23 °C. The procedure has been repeated discharging the battery in five steps, changing the current rate for each discharging process within two values. Also in this case, the climate chamber temperature has been set at 23 °C.
Table 4 shows a portion of the last part of the current tests variation.

Table 4: Portion of the test matrix for SOC influence investigation with two steps of current variation. Test done for ambient temperature of 23 °C

Nr.	Current [C rate]				
	100→80	80→60	60→40	40→20	20→Empty
25	5C	5C	5C	5C	1C
26	5C	5C	5C	1C	1C
27	5C	5C	1C	1C	1C
28	5C	1C	1C	1C	1C
29	1C	1C	1C	1C	5C
30	1C	1C	1C	5C	5C
31	1C	1C	5C	5C	5C
32	1C	5C	5C	5C	5C
33	1C	1C	1C	1C	1C
34	5C	5C	5C	5C	5C

In these tests the battery started in a fully charged state, and then it was discharged from 100% to

20% SOC with a current I_1, and from 20% SOC to the empty state (cut-off voltage) with a current I_2 different to I_1. As shown in the table, the tests are repeated decreasing the first ΔSOC step and inverting the current rate values. Also in this case, the tests were carried out for three different current rates (0.2C – 1C – 5C) and for an ambient temperatures of 23 °C.

2.2 Tests for Temperature Variation Dependency

The aim of the tests was to investigate the influence of the temperature variation during the discharge process on the total final capacity that the battery is able to deliver, and particularly to demonstrate if 1) this variation conditioned only the last part or the whole discharge process, and 2) if the aging state was a critical factor. Table 5 shows a resume of the tests.

Table 5: Test for temperature variation investigation with two temperature steps and 6 h pause in between. Test done for a current rate of 1C

Nr.	Temperature [°C]		
	100%→50%	Pause	50%→Empty
35	0	6 h	0
36	23		23
37	40		40
38	0		23
39	23		0
40	0		40
41	40		0
42	23		40
43	40		23

During each process, the battery started in a fully charged state, and then it was discharged from 100% to 50% SOC with a current of 1C at ambient temperature T_1, and from 50% SOC until the empty state (reaching of the cut-off voltage) with the same current, but a temperature T_2 different from T_1. The test was repeated with inverted two temperature values. The tests were carried out for three different temperatures (0 – 23 – 40 °C) and for two cells in different aged states. Between the two steps of the discharge process, a pause of 6 hours was set up, to temper the cell to the defined ambient temperature.

2.3 Test to Investigate the Presence of Pauses

The aim of the tests was to investigate the presence of pause of different length during the discharge process on the total final capacity that the battery was able to deliver, and particularly to demonstrate if 1) the length and 2) the aging state were critical factors. Table 6 shows a resume of the tests.

Table 6: Test for pause variation investigation. Test done for ambient temperature of 23 °C

Test Nr.			Pause duration
0.2C	1C	5C	
44	50	56	0 min
45	51	57	5 min
46	52	58	30 min
47	53	59	1 h
48	54	60	3 h
49	55	61	6 h

During each process, the battery started in a fully charged state, then it was discharged from 100% until 50% SOC with a current of I_1, and after a defined pause P, from 50% SOC until the empty state (reaching of the cut-off voltage) with the same current I_1. The tests were carried out for six different pause durations, and each one for three different current rates (0,2C – 1C – 5C). During all the tests, the climate chamber has been set with an ambient temperature of 23 °C.

In the following chapter, the results obtained during the tests are discussed and analysed, in order to try to explain the battery behaviour, especially focusing on the difference between the new and the aged cell.

3 Analysis of Results

In Table 2, Table 3, Table 4, Table 5 and Table 6, a resume of the test that will be discussed in the next subchapter of the work is shown. In each table, in the first column is reported the identification number of each test, which will be used as reference during the discussion. Before starting the analysis and discuss the obtained results, it is important to highlight a fundamental aspect: during the tests, the value of the total battery capacity taken as reference (i.e. discharge the battery from 100% SOC until the cutoff voltage with 1C current rate for an ambient temperature of 23 °C) has changed continuously, both for the new and aged battery. In particular, the value of the reference capacity has decreased for the aged battery, starting from an initial value of 7.207 Ah (90% of the nominal value) and terminating with a final value of 5.876 Ah (73.45% of the nominal value). In order to find an explanation of such behavior, support can be found in the results obtained from accelerated

aging test of the same cells used for this work (the detailed discussion of those tests is out of the goal of this paper): the cells have been aged cycling continuously with different current rate and depth of discharge (DOD) until they reached the end of life (EOL) criterion, and periodically a parameterization test has been done, in order to measure the actual battery capacity and the internal resistance. During these tests, the cells cycled for a temperature of 30 °C, with a current rate of 3C and depth of discharge (DOD) of 50% (around a SOC_{avg} of 50%) have shown more than 3000 equivalent full cycles before the end of life criterion. Taking this into account, the reason of the fast aging for the cells examined in this work (17% of capacity decreasing in less than 100 full cycles) cannot be found in normal lifetime degradation processes. We believe that some accelerated lithium plating phenomena have taken place during the charge and consequent discharge process at 0°C with current bigger than 1C. Concerning the new battery, the value of the reference capacity has changed from an initial value of 8.199 Ah (102.4% of the nominal value) to 8,802 Ah (110.02% of the nominal capacity). Taking into account that a formation process (three consequent full charge and discharge process with a current rate of 0,5C) has been carried out before the start of the planned tests when the battery was completely new, on the basis of the author experience increasing of capacity in such a great extent at the beginning of the lifetime has not yet been registered with this kind of cell. The supposition is that the cell is an oversized sample, whose full capacity has been completely released only after 50-60 equivalent full cycles. Moreover, increasing of capacity at the beginning of the lifetime can often be found in literature [12] [13], but it has not yet been fully explained and clarified. Nevertheless, in order to take into account this phenomenon both for aged and new battery, as soon as this behavior was detected, a measurement of the reference capacity under the above mentioned condition has been periodically carried out, in order to make the results in different conditions comparable among each other. The value of the reference capacity used in each test is not reported directly in this work. Following, the discussed results will refer to the relative total battery capacity. Moreover, because of the limited space, only the data that show the most interesting evidences are following discussed.

Figure 2 and Figure 3 show the result in terms of relative capacity respectively for cell A and cell B for the test carried out changing the current rate during the discharge process according to the procedure explained in 2.1.

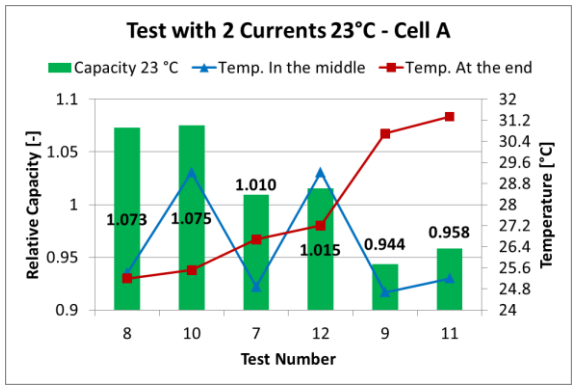

Figure 2: Total relative capacity for two step current for cell A at ambient temperature of 23 °C

As it can be seen, the first evident difference in terms of capacity value is basically due to the value of the current in the last part of the discharge process. As the discharge process has always been stopped when the cell has reached the cutoff voltage (2 V), it is clear that the bigger the current rate is, the bigger the contribute of the diffusion overvoltage at the end of the process is, that brings the cell to reach faster the voltage limit. This behavior seems to be valid for both cells in qualitative terms, although in the cell A the difference between the couple of tests 8&10 (end with 0,2C) and 7&12 (end with 1C) is bigger (6%) than the one of the cell B (2%). If the tests with same current rate at the end of the process are compared, one can see that the small difference in capacity is related to the value of the battery temperature when the current rate was changed (50% SOC) and at the end of the process.

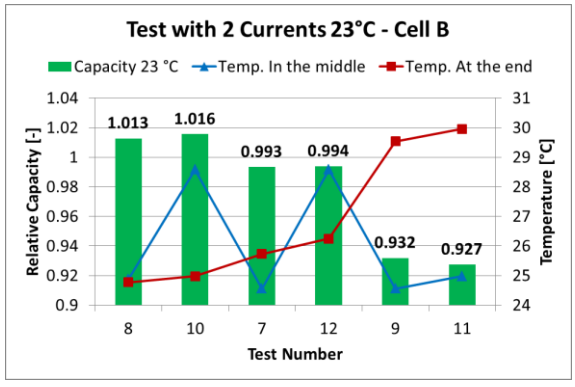

Figure 3: Total relative capacity for two step current for cell B at ambient temperature of 23 °C

Considering for example the tests 7 (0.2C – 1C) and 12 (5C – 1C), it can be noticed that the phase

at 5C current rate generated a temperature increase of 4 °C for cell A (from 24.8 to 28.8 °C) leading to an increase of final capacity of 0.5%. The same behavior can be found in Figure 3 for the cell B, although more limited quantitatively. Only the test 9 (0,2C – 5C) and 11 (1C – 5C) did not respect this trend for the cell B, despite the fact that the temperature in the middle and at the end of the discharge process was higher for the test 9 than for the 11. Nevertheless, as one could already expect, the temperature played a fundamental role, in the way that the current rate influenced not only the last part, but indirectly through the temperature the early discharge process. This behavior is not found in Figure 4 and Figure 5, where the results of the same tests are shown for an ambient temperature of 0 °C.

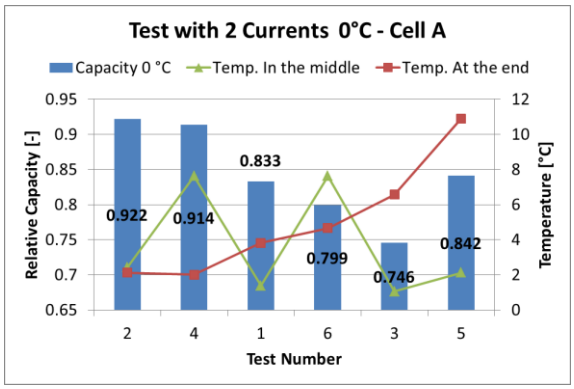

Figure 4: Total relative capacity for two step current for cell A at ambient temperature of 0 °C

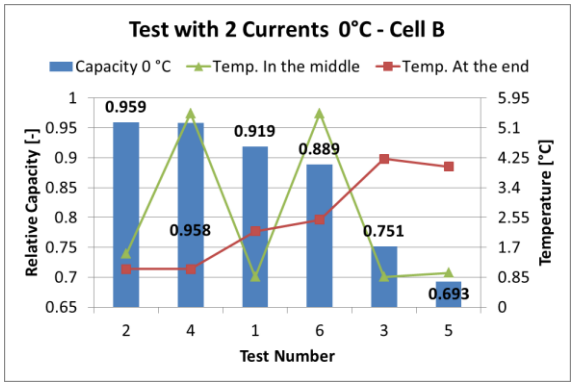

Figure 5: Total relative capacity for two step current for cell B at ambient temperature of 0 °C

In this case the deep ambient temperature effect joined with the high current rate could lead to difficulties during the diffusion process, making negligible the effect due to the increasing of the battery temperature in the middle of the discharge process. The same qualitative behavior was found for both cells, but once again with a clear difference in the test 3 (0,2C – 5C) and 5 (1C – 5C) between the two cells, showing that the presence of aging mechanisms change completely the battery behavior in terms of final battery capacity. As shown in Figure 6 and Figure 7, an accurate study of the same data for the ambient temperature of 40 °C show a trend similar to the one shown from the tests carried out for an ambient temperature of 23 °C: this can indicate that the battery aging state influence the beahviour of the cell only in some condition (test 9&11, 3&5 and 15&17), while temperature becomes a crucial parameter when its value starts to decrease below a certain limit (1&6 compared with 7&12 and 15&17).

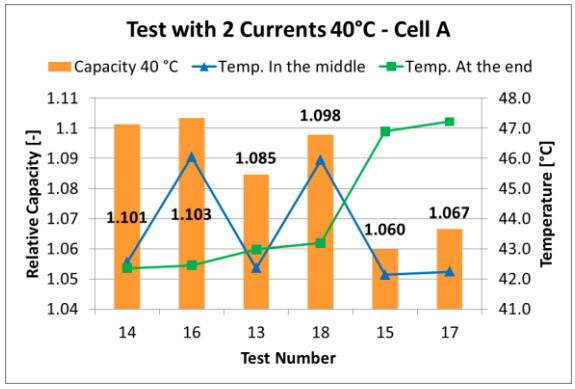

Figure 6: Total relative capacity for two step current for cell A at ambient temperature of 40 °C

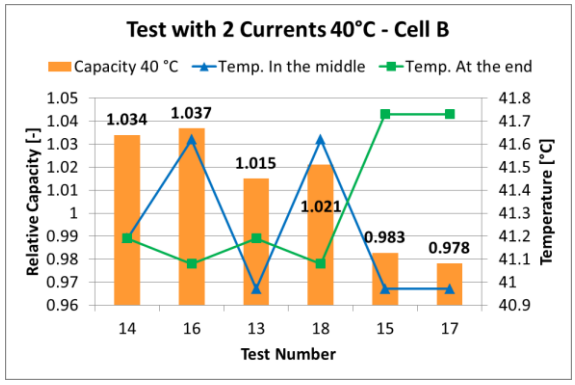

Figure 7: Total relative capacity for two step current for cell B at ambient temperature of 40 °C

The Figure 8 and Figure 9 show the current test discharging the battery in three steps with three different current rates and for an ambient temperature of 23 °C as explained in 2.1. Again in this case, the current rate in the last part of the process played an important role for both cells: in this case also the difference in quantitative terms between the couple of the tests seemed to be respected (e.g. difference 20&23 and 19&21 is between 5 and 7,5%).

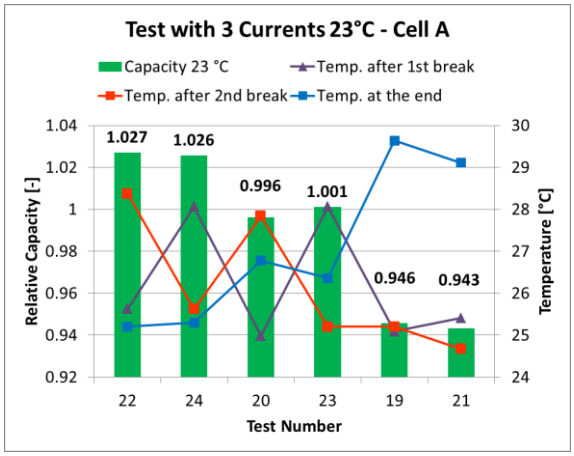

Figure 8: Total relative capacity for three step current for cell A at ambient temperature of 23 °C

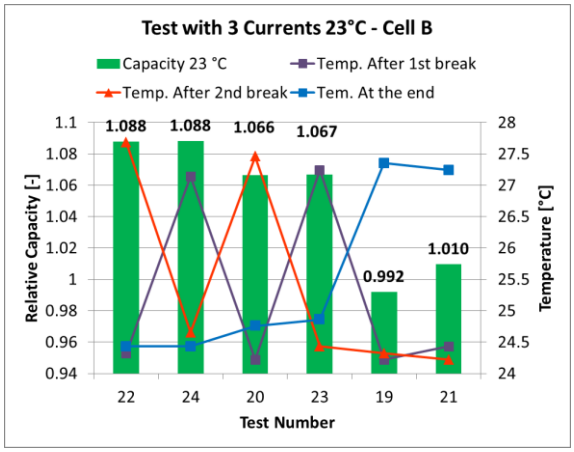

Figure 9: Total relative capacity for three step current for cell B at ambient temperature of 23 °C

Considering the tests in couple, based on the current rate in the last part of the process both for cell A and B, the difference between the values of the total capacity were negligible, a sign that the variation of the current in the early part of the process plays now a smaller role. Moreover, once more a different behavior between the cell A and B appeared for the tests terminating with 5C current. For the cell A the test 19 (0,2C – 1C – 5C) has shown more capacity than the test 21 (1C – 0,2C – 5C), while for the cell B the opposite has occurred: once more the influence of the aging phenomena when the cell is discharge with a high current rate in the last part of the discharge process could be seen comparing the two cells, but in respect of the previous discussion, the difference between test 19 and 21 is now for both cells negligible.

Figure 10 and Figure 12 show the results of the tests discharging the cells with two different values of current rate (1C and 5C), changing it for each test for different values of SOC.

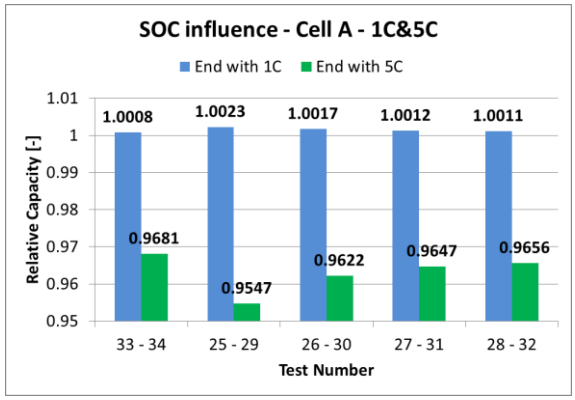

Figure 10: Total relative capacity for SOC influence investigation for cell A at ambient temperature of 23 °C

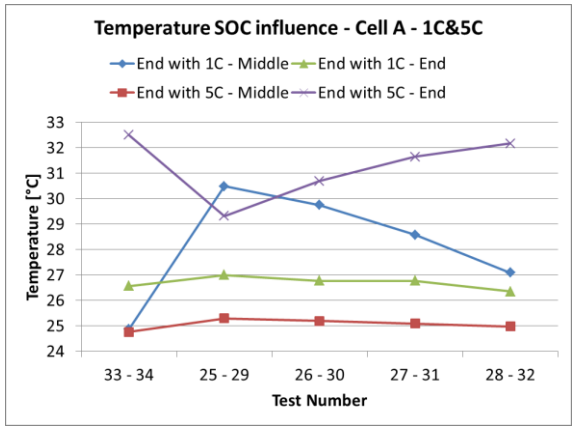

Figure 11: Battery temperature for SOC influence investigation for cell A at ambient temperature of 23 °C

The test are carried out two times, once starting with current rate I_1 (1C or 5C), second time with current rate I_2 (5C or 1C), as reported in Table 4. Both cells showed that the difference in final capacity was restrained when the discharge process started with 5C and terminated with a current rate of 1C, independently from when the current was changed. The small difference in capacity is due to the temperature value reached by the cells during the change of the current rate, especially when the 5C discharge process lasted longer (test 25 and 26): as shown in Figure 11 and Figure 13, for both cells a temperature between 30 and 31 °C during the change of the current rate led to a slight capacity increase at the end of the discharge process. An evident difference in the behavior can be observed when the discharge process started with a current rate of 1C and terminated with 5C. Both for cell A and B the maximum final capacity was reached when the discharge process was carried out completely with a constant current of 5C (test 34), mainly due to the higher temperature increase in respect to the

other tests, as shown in Figure 11 and Figure 13 (the temperature in the middle is the temperature at the beginning of the discharge process, as the current rate was never changed).

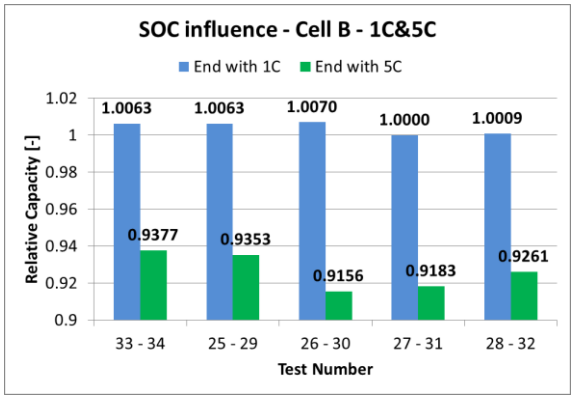

Figure 12: Total relative capacity for SOC influence investigation for cell B at ambient temperature of 23 °C

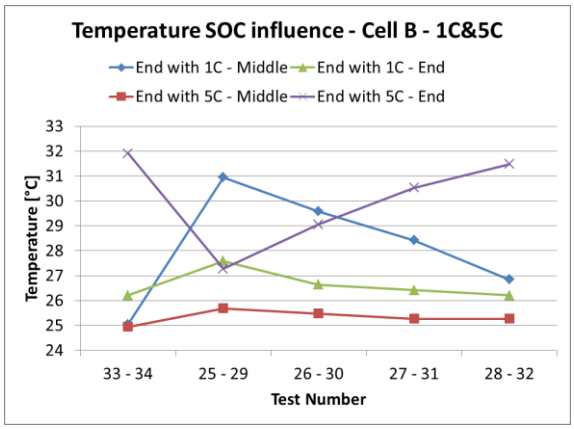

Figure 13: Battery temperature for SOC influence investigation for cell B at ambient temperature of 23 °C

In the rest of the tests (29-32), the bigger the discharge process with 5C current rate was, the higher was the final capacity, as the diffusion overvoltage at very low voltage did not influence the process. The beahvior was the same for both cells, except for the test 29, where cell B delivered more capacity as expected: the explanation of this cannot be found observing the battery temperature, as cell B reaches a temperature of 27 °C during test 29, evidently smaller in respect of the other tests where the discharge process with 5C lasted longer. It can be definitively stated, that the aging of the battery somehow modifies the weight of the temperature effect in respect to the effect that different current rates have in the diffusion process inside the cell, making one or another more important and more effective depending on the discharge process. A similar beahvior can be again found in results of other test configurations not reported in this work. Neverthless, more accurate and specific tests should be carried out in order to investigate some test configurations deeper, that produce different eveidences between new and aged cells. Figure 14 and Figure 15 show the value of the final capacity for both cells during the tests for temperature variation dependancy. As it can be clearly seen, the difference in the final capacity values appeared for the test where the last part of the discharge process was carried out with a temperature of 0 °C (35, 39 and 40).

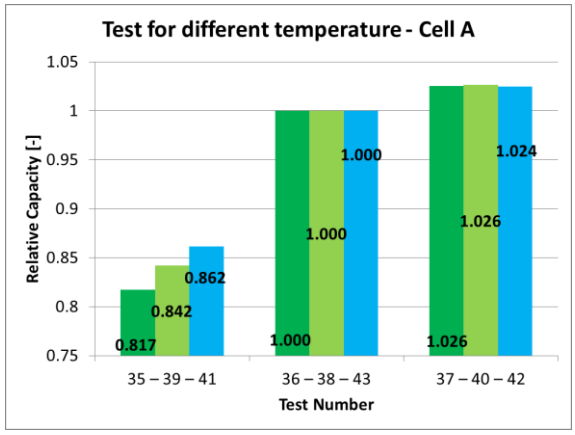

Figure 14: Total relative capacity for temperature influence investigation for cell A with a current rate of 1C

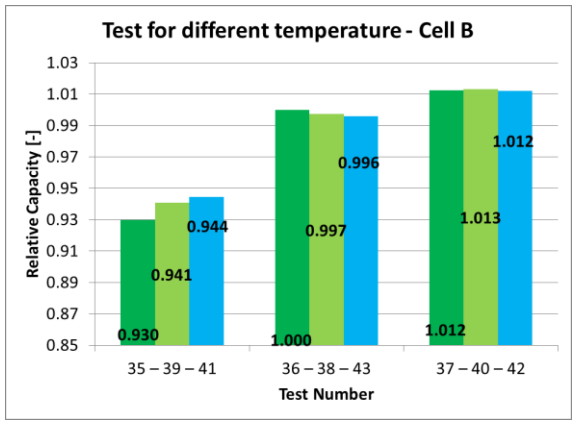

Figure 15: Total relative capacity for temperature influence investigation for cell B with a current rate of 1C

Between these tests, the difference in the capacity is due to the value of the battery temperature when the discharge process was firstly stopped (50% SOC): the biggest capaciy is either for cell A and B the one obtained in the test where the batteries were discharged from 100% until 50% SOC at 40 °C, followed by the one at 23 °C. Regarding the other six tests (the group 36, 38 and 43, and the group 37, 40 and 42) the ambient

temperature (and then the battery temperature) seemed to influence the final capacity value neither for cell A nor for cell B. By this it can be stated that the temperature variation during the discharge process has influence in the final battery capacity only if the difference between the two temperatures is significantly. Deeper investigations with frequent changes in the ambient temperature during the discharge process could give a better understanding of the phenomena.
Figure 16 and Figure 17 show the value of the final capacity for both cells during the investigation of the presence of pause of different length during the discharge process.

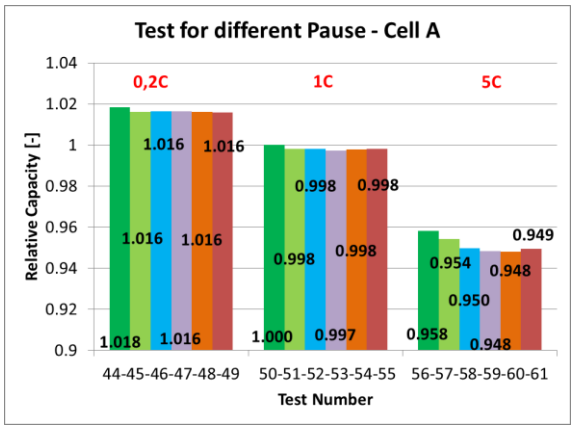

Figure 16: Total relative capacity for investigation of the presence of pause for cell A with different current rates

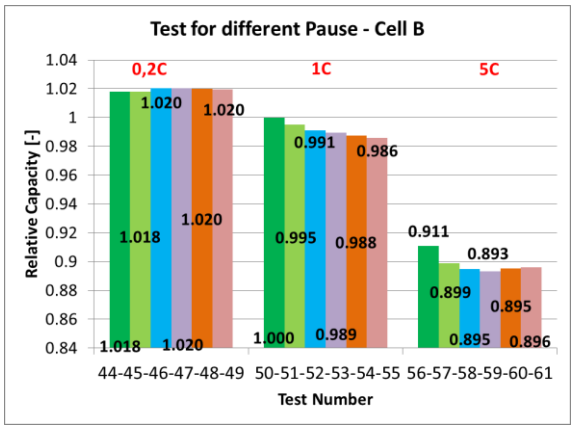

Figure 17: Total relative capacity for investigation of the presence of pause for cell B with different current rates

The presence of a break of different length (from 0 to 360 min) during the discharge process did not seem to influence the final capacity for both cells for a current rate of 0.2C. For cell A no big variation in terms of capacity is detected also for 1C current rate, while already small differences can be noted for cell B: the presence of a pause seemed to provoke a worsening in performance (test 50 → no pause, test 55 → 6 h pause). This can be seen more clearly for the tests done with 5C current rate (tests 56-61), both for cell A and B, where the discharging done without a break showed always a higher final capacity. One could think that the presence of a pause could be favourable for battery performance, allowing the completion of the diffusion processes in the cell, but in this case the tests have shown an opposite behavior. In the literature [14],[15] similar investigations can be found but only in terms of power capability: the authors have measured the impendance spectra of a battery during the relaxation process for different relaxation time and they have obtained an increasing battery internal resistance as the break time increased. For a deeper understading of the phenomena, tests at a higher current rate may be carried out, in order to highlight clearly the difference in final capacity.

4 Discussion: Influence on Online Capacity Estimation

The calculation of the actual capacity during the battery lifetime in EVs and PHEVs can be carried out in an easy way by an amp-hour throughput calculation between two defined SOC: starting from a defined SOC (for example SOC_{init} of 100%), the value of the final SOC_1 (1) calculated with the initial known capacity C_{actual} value is compared with the SOC_2 obtained with a methodology that does not use the known battery capacity (e.g. from the open circuit voltage (OCV) information, after a sufficient relaxation time has been spent).

$$SOC_1 = SOC_{init} + \frac{\int I(t) \cdot dt}{C_{actual}} \cdot 100 \qquad (1)$$

The difference between the SOC_1 and SOC_2 gives information about the actual battery capacity (2).

$$C_{actual} = \frac{\int I(t) \cdot dt}{SOC_{init} - SOC_2} \cdot 100 \qquad (2)$$

It is sufficiently clear that the value of the SOC_2 is not only dependent on the actual battery state, but also on the recently passed battery history: it is necessary to take into account what is happened during the discharge process in terms of current rate, temperature and pauses, as these factors influence the actual state of the battery and the performances during the whole discharge process. In this way the SOC_2 could be reformulated as following:

$$SOC_{2-real} = SOC_2 \cdot \alpha_I \cdot \alpha_T \cdot \alpha_{Pause} \quad (3)$$

where α_I, α_T and α_{Pause} are respectively the current factor, the temperature factor and the pause factor. It has to be considered that each factor has to be formulated differently, based on the obtained results. A possible implementation of the current factor is the following:

$$\alpha_{I-Total} = \prod \alpha_I^{\alpha_{SOC}} \quad (4)$$

$$\alpha_I = \frac{C_{I_1}}{C_{I_2}} \quad (5)$$

$$\alpha_{SOC} \propto \frac{1}{SOC} \quad (6)$$

In equation (4) the total current coefficient is calculated by the multiplication of the single current coefficients with the power of the actual SOC coefficient. From equation (5), the single current coefficients could be calculated from the ratio between the value of the final relative capacity that the battery could obtain if would be completely discharged with the actual current I_1 and the value of the final relative capacity that the battery could obtain if would be completely discharged with the actual I_2 in the precedent time step of the calculation. From equation (6), the value of the SOC coefficient could be obtained taking into account that the effect of the current rate increases with the decreasing of the SOC value, as already discussed in the test explanation in chapter 3. Similar procedure could be followed to obtain the coefficient for the temperature variation dependency and the one relative to the pause, considering that to obtain more precise calculation of the total battery capacity, ulterior investigations regarding these two factors are needed.

It is also clear that, in order to use this methodology to calculate the actual battery capacity, the use of the OCV information to obtain the SOC_2 can be carried out only if the cell is in a state in which the OCV in respect to the SOC is not flat. Another problem regards the changing of the OCV curve of $LiFePO_4$ cells during lifetime: in order to make sure that the value of the actual capacity is correctly calculated, algorithms able to adapt online the value of the relaxation voltage curve based on the degradation history of the cell have to be present in a complete BMS.

5 Conclusion

In this paper a complete investigation of the behavior of a $LiFePO_4$ cell in terms of final battery capacity during the discharge process, in new and aged state, changing the value of the current, temperature and pause is discussed. The cell has maintained the same behavior during the battery lifetime, except for some extreme conditions: the two cells have showed completely different behavior during the discharge process carried out with the sequence 0.2C - 5C and 1C - 5C, sign that the aging state can influences the battery performance in some particular operation. The same behavior has been found when the current rate has been changed more frequently. The presence of pause seemed also to influence the final battery capacity: the cells have shown slightly differences during the tests, especially for high current rate, but clearer information could be obtained discharging the cell with higher current rate. The temperature dependency tests did not shown relevant evidences in terms of difference between the two cells; influences in the battery total capacity could be found when the last part of the discharge process was carried out at 0°C. In order to obtain more knowledge in terms of temperature dependency, additional investigations should be carried out, e.g. varying the value of the temperature more frequently during the discharge process. In future analyses, the tests should be done trying to influence the lifetime of the battery as less as possible, so that the battery total capacity does not decrease significantly.

Acknowledgments

This work was kindly financed by the German Federal Ministry for Education and Research within the project Powerblock+.

References

[1]. B.A. Johnson, R.E. White, *Characterization of commercially available lithium-ion batteries,* Journal of Power Sources, 70 (1998), 48-54.

[2]. W.X. Shen, C.C. Chan, E.W.C. Lo, K.T. Chau, *Estimation of battery available capacity under variable currents*, Journal of Power Sources, 103 (2002), 180-187.

[3]. M.A. Roscher, J. Vetter, D.U. Sauer, *Cathode material influence on the power capability and utilizable capacity of next generation lithium-ion batteries*, Journal of Power Sources, 195 (2010), 3922-3927.

[4]. Zhang et al., *Method for battery capacity estimation*, United States Patent Application Publication, Pub. No.: US 2009/032283 A1, Dec. 31, 2009.

[5]. M. Einhorn, F.V. Conte,C. Kral, J. Fleig, *A Method for Online Capcity Estimation of Lithium Ion Battery Cells Using the State of Charge and the Transferred Energy*, IEEE Transactions on Industry Applications, Vol. 48, NO. 2, March/April 2012.

[6]. G. Plett, *Recursive approximate weighted total least squares estimation of battery cell total capacity*, Journal of Power Sources, 196 (2011), 2319-2331.

[7]. X.Tang, X. Mao, J. Lin, B. Koch, *Capacity Estimation for Li-ion Batteries*, American Control Conference, San Francisco, USA, June/July 2011.

[8]. B. Rosca, J.T.B.A. Kessels, H.J. Bergveld, P.P.J. van den Bosch, *On-Line Parameter, state-of-Charge and Aging Estimation of Li-ion Batteries*, IEEE Vehicle Power and Propulsion Conference, Seoul, Korea, Oct. 9-12, 2012.

[9]. Y. Zheng, L. Lu, X. Han, J. Li, M. Ouyang, *$LiFePO_4$ battery pack capacity estimatio for electric vehicles based on charging cell voltage curve transformation*, Journal of Power Sources, 226 (2013), 33-41.

[10]. http://www.digatron.com/de/legal-notice/gtc/

[11]. http://www.binder-world.com/en/

[12]. M. Dubarry, V. Svoboda, R. Hwu, B.Y. Liaw, *Capacity and power fading mechanism identification from a commercial cell evaluation*, Journal of Power Sources, 165 (2007), 566-572.

[13]. M. Kassen, J. Bernard, R. Revel et al., *Calendar aging of a graphite/$LiFePO_4$ cell*, Journal of Power Sources, 208 (2012), 296-305.

[14]. D. Andre, M. Meiler et al., *Characterization of high-power lithium-ion batteries by electrochemical impedance spectroscopy. I. Experimental investigation*, Journal of Power Sources, 196 (2011), 5334-5341.

[15]. W. Waag et al., *Experimental investigation of the lithium-ion battery impedance characteristic at various conditions and aging states and its influence on the application*, Applied energy, 102 (2013,) 885-897.

Authors

Andrea Marongiu received his master degree in Electrical Engineering from the Cagliari University, Cagliari, Italy, in 2010. In March 2011 he joined the Institute for Power Electronics and Electrical Drives (ISEA) by the RWTH Aachen University, Aachen, Germany, as a research associate. His areas of interest are EV batteries and the related on board Battery Management System with a special focus on $LiFePO_4$ cells.

Thapakorn Pavanarit studies Electrical Engineering at the RWTH Aachen University, Aachen, Germany. Since 2012 he has been working as a Student assistant at the Institute for Power Electronics and Electrical Drives (ISEA). He has finished his Master degree in April 2013.

Dirk Uwe Sauer received his diploma in Physics from University of Darmstadt in 1994 and the Ph.D. degree from Ulm University, Ulm, Germany, in 2003. From 1992 to 2003, he was a Scientist at Fraunhofer Institute for Solar Energy Systems, Freiburg, Germany. In October 2003, he was a Junior Professor, and since 2009 he has been a Professor at RWTH Aachen University, Aachen, Germany, for Electrochemical Energy Conversion and Storage Systems.